*Monikandon Sukumaran[2], Ravisankar Natarajamani[1]**

[1]Department of Civil Engineering, Faculty of Engineering and Technology, Annamalai University, Tamil Nadu, India, [2]Research Scholar, Department of Civil Engineering, Faculty of Engineering and Technology, Annamalai University, Tamil Nadu, India

Scientific paper
ISSN 0351-9465, E-ISSN 2466-2585
https://doi.org/10.62638/ZasMat1142

Zastita Materijala 66 (2)
225 - 232 (2025)

Inhibition of marine corrosion of thermo mechanically treated rod using green synthesized iron oxide nanoparticles

ABSTRACT

The present study investigates the use of iron oxide nanoparticles synthesized from Ficus tsjahelas a protective coating for Thermo Mechanically Treated(TMT) rods in amarine environment. The method startedwith the extraction of theinhibitor from plant leaves using ethanol, followed by the preparation of iron oxide nanoparticles. Then (TMT) rods were coated with these FeNPs and exposed to thecorrosive conditions of marine environment. In this study iron oxide nanoparticles were produced using chemical precipitation approach and the particle size effects are fully studied by applying techniques such as Fourier transform infrared spectroscopy (FT-IR), ultraviolet visible spectroscopy (UV-Visible) and SEM. Interestingly when (TMT) rods were coated with 10 layers of FeNPs, the corrosion inhibition efficiency increased to 94.1% for 8mm rods, 95.4% for 10mm rods and 98.7% for 16mm rods respectively. Furthermore, the inhibitive results corresponded with the Langmuir adsorption isotherm indicating that the inhibitory effect of FeNPs follows a physical adsorption process.

Keywords: *nanoparticles; green nanoparticles; marine structure corrosion;TMT rod Corrosion; brackish water corrosion.*

1. INTRODUCTION

Metals and alloys remain highly versatile engineering materials for structural applications. However, metal alloys can corrode and lose their mechanical properties when exposed to the corrosive environments [1-4]. Corrosion is a significant environmental threat, impacting not only the economy but also on resource conservation and safety across various engineering fields, including construction, chemical processing, automotive, mechatronics, metallurgy and the medical industry [5].

Corrosion costs approximately 4% of the world's GDP or one-fifth of global steel production in offsettinglosses caused by corrosion [6,7]. In reinforced concrete structures, corrosion reduces the cross-sectional dimension of the reinforcement and causes volume changes in corroded materials, compromising the structural stability [8-14].

The corrosion of steel bars weakens concrete structures, leading to stability problems [15]. Corrosion inhibitors are a practical alternative due to their ease of use and cost-effectiveness in protecting the passive layer from corrosion damage [16]. These inhibitors are both inexpensive and efficient at controlling material deterioration [17, 18, 19].

Corrosion inhibitors work by forming an invisible oxide film on the material's surface, preventing corrosive substances from reaching the metal and inhibiting oxidation or reduction reactions, making dissolved oxygen ineffective. Various inorganic and organic inhibitors are used in the metal industry to minimize corrosion. Inorganic inhibitors are used less frequently because they tend to be costly and pose risks to both the environment and human health. In contrast, nanomaterials serve as efficient corrosion inhibitors due to their higher surface-to-volume ratio compared to traditional macroscopic materials [20,21, 22].

Metal nanomaterials have attracted researchers' *interest* for potential applications in environmental, medicinal, and electrochemical sciences [23-26]. The synthesis of nanoparticles

*Corresponding author: Ravisankar Natarajamani
E-mail: ravisankarnatarjamani71@gmail.com
Paper received: 19.06.2024.
Paper corrected: 28.08. 2024.
Paper accepted: 12.09.2024.

using physical and chemical methods is restricted due to their significant toxicity [23-29] and the high cost of the chemicals involved [26]. On the other hand using plant extracts to produce nanoparticles is a more cost-effective and efficient approach as the phytochemical compounds present can reduce and stabilize metal ions, leading to the formation of metallic nanoparticles.

In this context, the present study explores the use of green-synthesized iron oxide nanoparticles to reduce marine corrosion of vital structural elements such as Thermo-Mechanically Treated (TMT) rods. Because oftheir environmentally friendly production methods and inherent corrosion resistance, iron oxide nanoparticles show great potential for enhancing the durability and lifespan of TMT rods in marine environments. This study represents a significant step towards long-term corrosion mitigation strategies that align with the current need for environmental sustainability.

2. MATERIALS AND METHODS

Inhibitor Preparation

In the process of making the inhibitor, 2 kilograms of freshly obtained *Ficus tsjahela* (F) leaves from the Nagapattinam district were used. These leaves were dried for two weeks in the shade and then pulverized. The pulverized leaves were placed in a thimble and then inserted into the Soxhlet extractor. A 500 milliliter round-bottom flask with a condenser was attached to the Soxhlet extractor , which was filled with an 85% ethanol-water solution. The setup was placed on a mantle, allowing the solvent to evaporate and pass through the Soxhlet extractor to condense.

When the solvent had condensed, droplets that formed dripped from the Soxhlet extractor into a small container containing the plant material. Once the solution reached the siphon, the resulting solution was returned to the round-bottom flask. This process was carried out for one hour, after which the extracted solution was allowed to cool to room temperature. The concentrated substance was then processed using a rotary evaporator and filtered through Whatman No. 1 filter paper. The experiment was repeated three more times with the same sample within the thimble, each utilizing 500 milliliters of the solvent combination.

The crushed leaves were placed in a thimble, which was then inserted into the Soxhlet extractor. A 500 mL round-bottom flask, connected to a condenser, was filled with an 85% ethanol-water mixture and attached to the extractor. The setup was placed on a heating mantle, causing the solvent to evaporate and pass through the Soxhlet extractor into the condenser. Once condensed, the solvent started trickling into the extractor and interacting with the plant material within the thimble. Once the solvent level surpassed the siphon, it was transferred into the round-bottom flask, and the cycle was repeated for an hour. The extracted solution was cooled to room temperature. This procedure was repeated three more times, each using 500 mL of fresh solvent mixture for the same sample [20-21, 29-33].

The filtrate was concentrated in a vacuum chamber, yielding a material approximating green oil that was then kept in the refrigerator for future use. It is interesting to note that when exposed to Fe^{3+}, Mg-HCl, and NaOH, the crude extract changed hues to green, orange-red, and yellow. In addition, underUV light, the crude extract showed a purple mark, while treatment with ammonia turned it yellow. Molisch's reagent, which consists of α-naphthol in ethanol, was applied to a pinch of the sample, followed by a few droplets of concentrated H_2SO_4, resulting in a purple colour and verifying the existence of flavones, which are glycosides.

Iron Oxide Nanoparticles (FeNPs) Preparation:

A solution with a concentration **of** 0.01 M ferrous sulphate heptahydrate was prepared by mixing 70% water and 30% ethanol to make 100 mL of FeNPs. This combination was then thoroughly mixed with 50 mL of a 0.01% crude extract solution. Following a three-hour reaction time, 50 mL of 0.01% extract was added drop by drop and mixed for another 25 minutes. The generated particles were then separated by centrifugation and carefully cleaned using double-distilled water and ethanol. The FeNPs were vacuum-dried at room temperature for a whole day before being kept in ethanol until use.

Characterization of FeNPs

To analyze the green iron nanoparticles synthesized, FT-IR (JASCO FTIR-4100) and UV-visible spectrophotometry (JASCO V-630) were employed. In addition, the surface texture and chemical content of the particles were determined using scanning electron microscopy combined with energy-dispersive spectroscopy (SEM-EDS) (Hitachi-S 3400N).

Weight Loss Measurements

Weight loss assessments were carried out in line with prior studies [29-31]. To provide **a** basic introduction, TMT rods of three different sizes 8 mm, 10 mm and 16 mm with a length of 5 cm were abraded with emery sheets ranging in grade from 600 to 1200. The steel rods were then carefully cleaned using distilled water and acetone. Every rod was subsequently allowed to air dry at room temperature and then weighed. A solution of iron nanoparticles (FeNPs) at a concentration of 100

parts per million was prepared in acetone. The inhibitor was then applied as a coating using a brush at three different concentrations: 1, 5, and 10, on TMT rods with diameters of 8 mm, 10 mm, and 16 mm. The weight of the TMT rod was recorded after coating. The coated rods were then placed in brackish water for 2 hours at 303 K. After the incubation period, the samples were gently rinsed with water, followed by acetone, and allowed to air dry. The weight of the sample was then measured. According to the estimations, each coating for the TMT rod required 1 mL of 100 ppm FeNPs solution. After every coating, the 8 mm, 10 mm, and 16 mm rods were allowed to dry for 10 minutes at room temperature. In this work, TMT rod pieces with dimensions ranging from 8 mm, 10 mm, and 16 mm were used with the following chemical composition: C, 4.93%; Mn, 1.09%; Si, 1.78%; and the other constituents mostly Fe.

Equations 1-2 were used to calculate inhibiting efficiency (%IE), corrosion rate (CR) and surface coverage (θ).

$$IE(\%) = \frac{(W_2 - W_1)}{W_2} \times 100 \quad (1)$$

$$\theta = \frac{(W_2 - W_1)}{W_2} \quad (2)$$

W_2 and W_1 represent the specimens weight prior to and post-incubation in marine environment.

3. RESULTS AND DISCUSSION

Analysis of crude extract and FeNPs

UV-visible spectroscopy has been employed to evaluate the characteristics of both the raw extract and FeNPs. In particular, the crude extract showed two unique spectral bands at 273 nm and 279 nm, indicating the presence of flavones [24, 29, 30]. The alcoholic extract from the leaves of *Ficus tsjahela* was found to contain substantial amounts of phenolic compounds and tannins [34]. FeNPs, on the other hand, showed a distinct band around 369 nm, implying that this property may be due to the nanoparticles themselves.

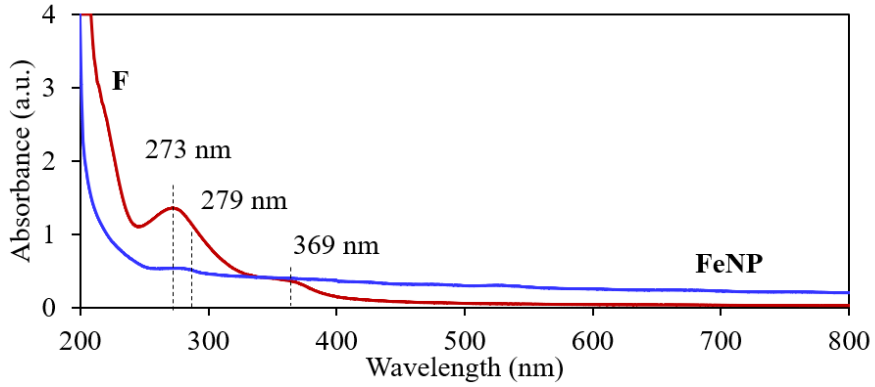

Figure 1.UV-visible spectrum for F and FeNPs

FT-IR spectra shown in Fig. 2 indicated distinct peaks in the crude extract corresponding to the stretching vibrations of -O-H, -C-H, -C=O, and -C-O at 3533 cm^{-1}, 3268 cm^{-1}, 1637 cm^{-1}, and 1384 cm^{-1}respectively. For the FeNPs, distinct peaks showing metal-oxygen interactions were identified at 507 cm^{-1} [29-31]. Fig. 3 displays the FeNPs' morphologies. FeNPs have a mean diameter of 155 ± 23 nm. The SEM-EDS spectrum was used to identify the nanoparticles' elemental composition, with carbon 39%, oxygen 19%, phosphorus 6%, sulphur 5%, and the rest iron as the main constituent.

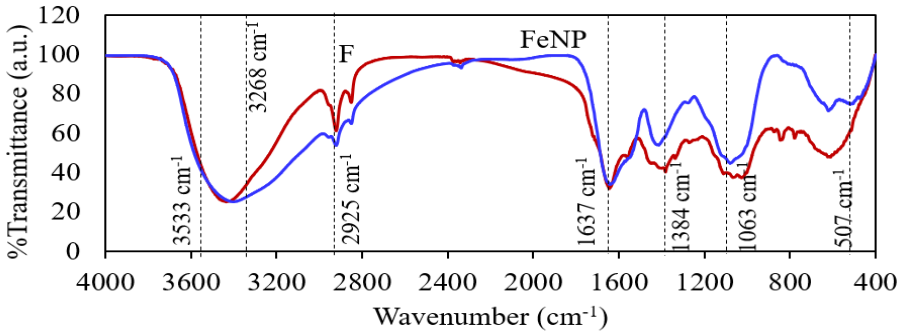

Figure 2.FT-IR spectrum of F and FeNPs

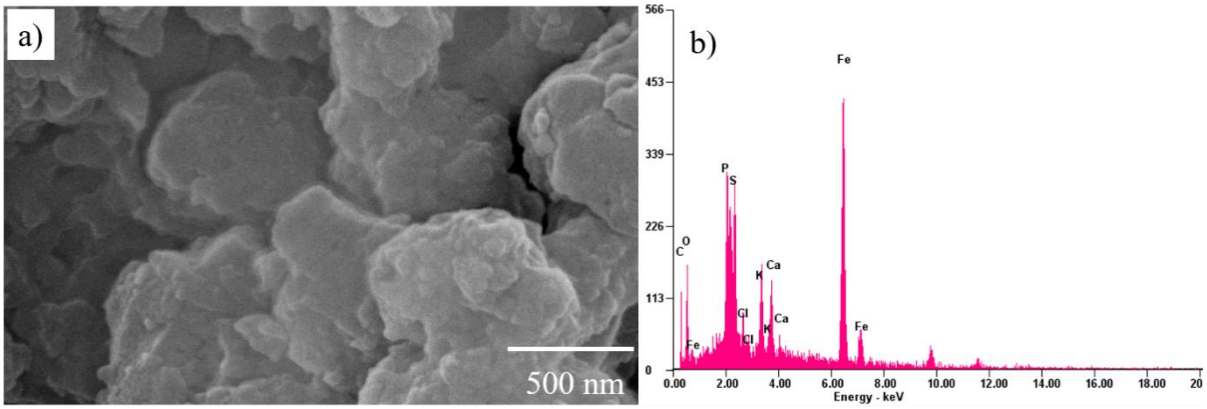

Figure 3.(a) Morphology of iron oxide nanoparticles by SEM and (b) EDS.

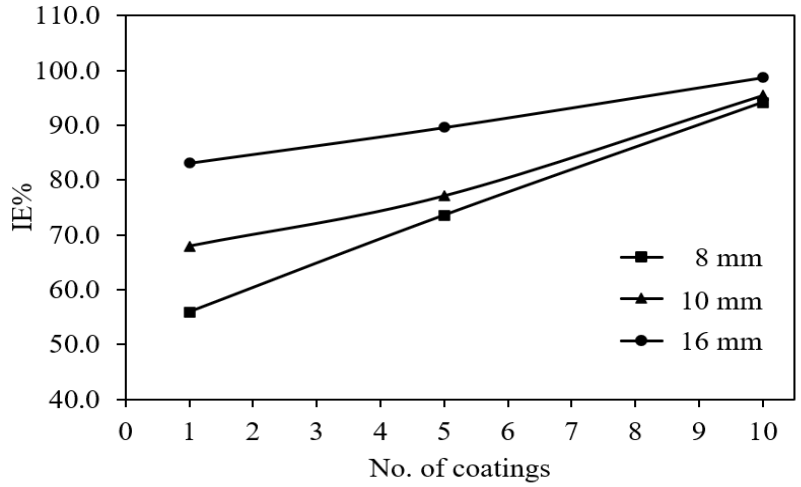

Figure 4.FeNPs effectiveness in inhibiting corrosion of TMT rods on brackish water

Table 1.Corrosion inhibition efficacy of FeNPs and thermochemical properties.

Coating	Weight loss (mg/h)	IE%	Surface Coverage (θ)	Corrosion Rate (mm/y)	K (KJ/mol)	ΔG(KJ/mol)
8 mm rod						
1	1.5	55.9	0.5588	0.7886	633.3333	-16090
5	0.9	73.5	0.7353	1.0376	277.7778	-14034
10	0.2	94.1	0.9412	1.3282	800.0000	-16673
10 mm rod						
1	1.4	67.9	0.6794	0.9587	1059.5238	-17374
5	1.0	77.1	0.7710	1.088	336.6667	-14514
10	0.2	95.4	0.9542	1.3465	1041.6667	-17331
16 mm rod						
1	1.3	83.0	0.8304	1.1719	2448.7179	-19463
5	0.8	89.6	0.8957	1.2639	858.3333	-16848
10	0.1	98.7	0.9870	1.3928	3783.3333	-20548

ΔG_{ads} -The free energy of adsorption; K – adsorption equilibrium constant.

$$\Delta G_{ads} = -RT \ln (55.5\, K_{ads}) \quad (3)$$

where R is the gas constant (8.314 J K^{-1} mol^{-1}), T is the absolute temperature, 55.5 is the concentration of water in the solution, K_ads is the equilibrium constant, and ΔG_ads is the free energy of adsorption. Using the corrosion parameter of surface coverage (θ) [23-24], the

adsorption behaviour of inhibitor *Ficus tsjahela* on TMT rod in brackish water was studied using Langmuir and Temkin isotherms plots. Below are the mathematical equations 4-5 for the Langmuir and Temkin isotherms.

$$K = \frac{\theta}{1-\theta} \times \frac{1}{C} \quad (4)$$

$$K_{ads}C = ex^{f\theta} \quad (5)$$

Corrosion rate =W/DAT mm/year.

Where,

W – Weight loss (mg)

D- Density of the specimens for TMT rod 7.87 g/cm^3

T- Time of exposure in hour

Area of specimen (mm^2)

Langmuir adsorption isotherm assumes a monolayer adsorption onto a surface with a finite number of identical sites. The equation is

$$\frac{q_e}{q_m} = \frac{K_L C_e}{1+K_L C_e} \quad (6)$$

Or equivalently

$$C_e \frac{q_e}{q_m - q_e} = \frac{1}{K_L q_m}$$

Where,

$q_e$represents the quantity of adsorbate adsorbed in every unit mass of adsorbent in equilibrium.

$q_m$represents the maximal adsorption capacity.

$C_e$is the adsorbate's equilibrium concentration in solution

$K_L$the Langmuir constant equates to the affinity of binding sites

Temkin adsorption isotherm takes into consideration how adsorbate-adsorbte interactions affect the adsorption process. The equation is given below:

$$q_e = B\ ln(AC_e) \quad (7)$$

Where

$$B = \frac{RT}{b}$$

and

$$ln(q_e) = ln(A) + \frac{bC_e}{RT}$$

Freundlich isotherm for adsorption explains absorbance on heterogeneous surfaces that suggests that adsorption capacity increases as concentration gets higher. The equation

$$q_e = K_F C_e^{\frac{1}{n}} \quad (8)$$

Where,

$q_e$represents the quantity of adsorbate adsorbed in every unit mass of adsorbent in equilibrium.

$C_e$is the adsorbate's equilibrium concentration in solution.

$K_F$corresponds to the Freundlich constant, which is related to adsorption capacity.

$\frac{1}{n}$The adsorption intensity is associated with the Freundlich exponent.

TheFeNPs effectiveness was rigorously examined by applying them to TMT rods of varied diameters 8 mm, 10 mm, and 16 mm with the numbers of coatings being1, 5, and 10. This assessment was conducted in a brackish water environment with **a** salinity of 5 ppt. TMT rods with FeNPs coatings and their uncoated counterparts were thoroughly examined. Figure 4 depicts a clear association between the quantity of FeNP coatings and the resulting percentage of inhibiting efficiency (%IE).

For 8 mm TMT rods, the inhibitor originally had an %IE of 55.9%**,** which increased to the notable value of 73.5% after five coatings. After 10 coating applications to the TMT rod, an outstanding %IE of 94.1% was attained. When using 10 mm TMT rods, the efficiency of FeNPs began at 67.9% for the initial coatings and steadily grew to an astounding 77.1% after five coatings, ending with a remarkable 95.4% inhibition after 10 coatings. The inhibition efficacy of FeNPs on 16 mm TMT rods ranged from 83.0% after one coating to 89.6% after five coatings, with an impressive 98.7% inhibition effectiveness after ten coatings. It was notable that FeNPs efficiently coated the whole surface of the TMT rod. In addition, as the diameter of the rod increased, the surface area expanded and the corrosion inhibitory capability of FeNPs appeared to rise. It is worth noting, however, that adding more FeNPs coatings did not result in a substantial rise in %IE. The adsorption behaviour of FeNPs provides significant insights into the corrosion prevention process. Fig. 3 shows the weight loss data. Particularly, correlation coefficient values were calculated to offer an understanding of the performance of FeNPs.

Fig. 5b depicts the Temkin adsorption isotherm, which shows nonlinear interactions. The correlation

coefficients were 0.9637 for the 8 mm TMT rod, 0.9147 for the 10 mm rod, and 0.9487 for the 16 mm rod. Fig. 5c depicts the non-linear correlations of the Freundlich adsorption isotherm, with correlation coefficient values of 0.9810 for the 8 mm TMT rod, 0.9315 for the 10 mm rod, and 0.9561 for the 16 mm rod. Fig. 5a shows that FeNPs from F performed well in the Langmuir adsorption isotherm, with coefficients of correlation values of 0.9900 for the 8 mm rod, 0.9917 for the 10 mm rod, and 0.9986 for the 16 mm TMT rod respectively. This shows a better adsorption process for FeNPs from F when using the Langmuir model. Previous investigations [4, 21, 31] have suggested that the process of inhibition is due to the inhibitor's adsorption on the TMT surface. The enhanced inhibitive performance provided by the inhibitor is most probably owing to the presence of heteroatoms plus electrons in natural products, as well as their larger molecule size, allowing for better coverage of the metal's outer surface area.

Corrosion inhibition generally takes place through adsorption, which can involve physisorption, chemisorption, or a combination of the two. In this research, the Langmuir adsorption isotherm showed correlation coefficient values near unity, indicating that the inhibition mechanism aligns with physisorption, chemisorption, or both types of adsorption.

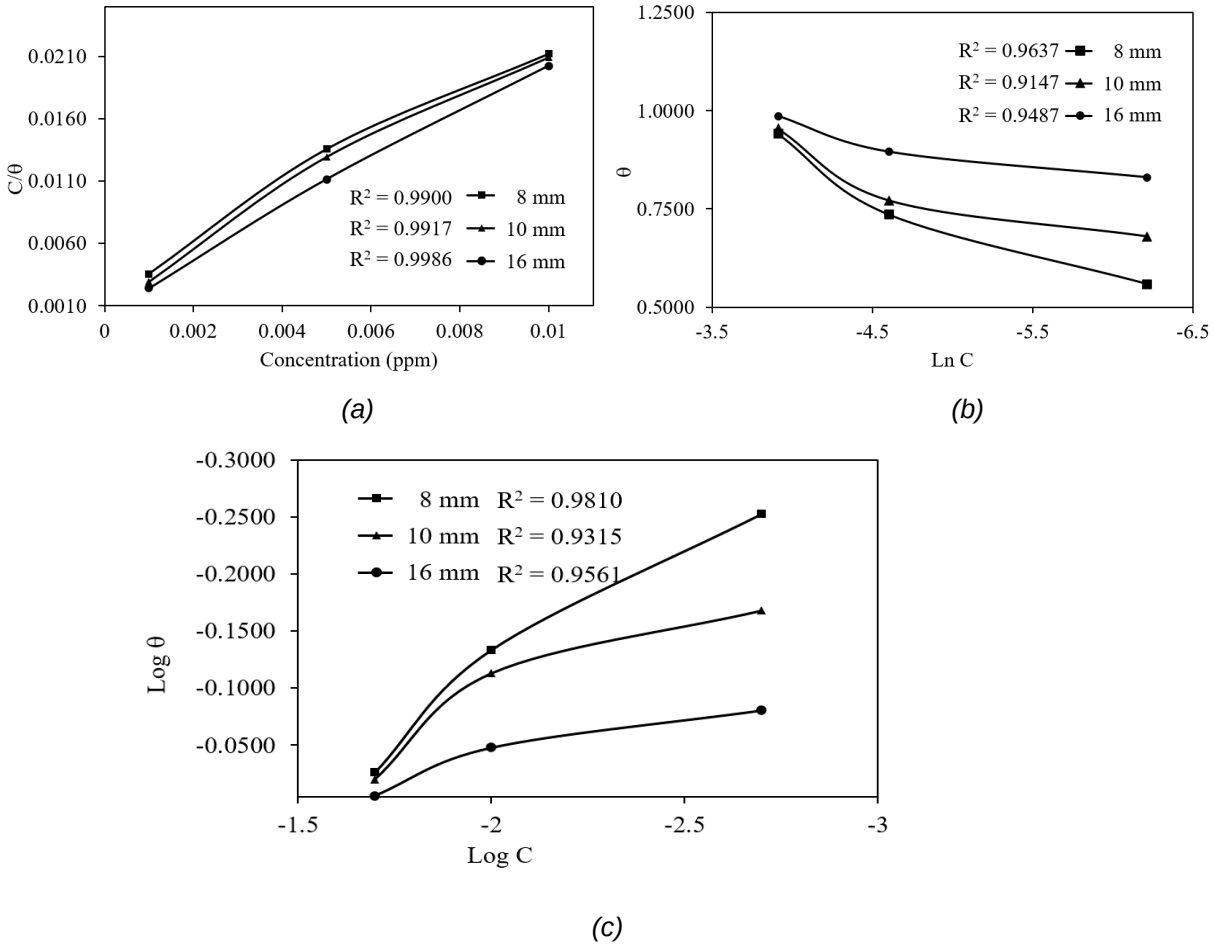

(a) *(b)*

(c)

Figure 5. (a) Langmuir, (b) Temkin and (c) Freundlich adsorption isotherms of biogenic FeNP-mediated corrosion inhibition of TMT rods in brackish water

5. CONCLUSION

In response to increased worries about the adverse ecological and economic consequences of corrosion, there is an emphasis on finding sustainable, cost-effective, and efficient corrosion inhibitors. This work delves into the field of eco-friendly inhibitors, revealing the extraordinary potential of iron oxide nanoparticles (FeNPs) prepared from *Ficus tsjahela* leaves.

The adhesion of *Ficus tsjahela* FeNPs to the Langmuir adsorption isotherm during adsorption provides important insights into the molecular interactions that drive corrosion inhibition. Advanced microscopy techniques, particularly scanning electron microscopy (SEM) and energy-dispersive spectroscopy (EDS)**,** provide substantial evidence supporting the efficacy of this corrosion protection technology. This study demonstrates the potential

for the transformation of green-synthesized FeNPs generated from *Ficus tsjahela* leaves as a viable answer in the ongoing war against corrosion.

Acknowledgement

Monikandon Sukumaran thankTamil Nadu Dr.J. Jayalalithaa Fisheries University Nagapattinam and Annamalai University, Chidambaram for motivating to do research.

6. REFERENCE

[1] B.A.Shaw, R.G.Kelly, (2006) what is corrosion? Electrochem. Soc. Interface., 15, 24–26. https://doi.org/10.1149/2.f06061if

[2] A.Singh, E.E. Ebenso, M.A.Quraishi, M. Mobin, M. Rizvi, M (2012) Corrosion inhibition ofcarbon steel in HCl solution by some plant extracts. Int. J. Corros.,Article ID 897430. http://dx.doi.org/10.1155/2012/897430.

[3] G.F.Hays., (2010) Now is the Time. https://www. scientific.net/AMR.95.-2.pdf (Accessed on 02 June, 2024).

[4] D. Valença, K.G.B. Alves, C.P. de Melo, N. Bouchonneau (2015) Study of the efficiency of polypyrrole/ZnO nanocomposites as additives in anticorrosion coatings. Mater. Res, 18(2):273–278https://doi.org/10.1590/1516-1439.371614

[5] S.K.Sharma, P.Anjali, O.L.Bassey,(2015) Potential of *Azadirachta indica* as a green corrosion inhibitor against mild steel, aluminum, and tin: a review. J Anal Sci Technol. 6,26. https://doi.org/10.1186/s40543-015-0067-0

[6] S.A. Umoren, M.M.Solomon, (2014) Recent developments on the use of polymers as corrosion inhibitors: a review. Open Mater. Sci, 8(1):39–54. DOI**:** 10.2174/1874088X01408010039

[7] J.Weber, (1983) Current corrosion protection problems. Mater. Des, 4(2):723–727 https://doi.org/10.1016/0261-3069(83)90137-1

[8] K.Andisheh, A.Scott, A.Palermo, (2016) Seismic Behaviour of Corroded RC Bridges: Review and Research Gaps. Int. J. Corros. 3075184. https://doi.org/10.1155/2016/3075184

[9] K.Andisheh, A.Scott, A.Palermo, D.Clusas, (2019) Influence of chloride corrosion on the effective mechanical properties of steel reinforcement. Struct. Infrastruct. Eng. *15*, 1036–1048. https://doi.org/10.1080/15732479.2019.1594313

[10] R.A.Hawileh, J.A. Abdalla, A.Al Tamimi, K. Abdelrahman, F.Oudah, (2011) Behavior of Corroded Steel Reinforcing Bars Under Monotonic and Cyclic Loadings. Mech. Adv. Mater.Struct., *18*, 218 -224. https://doi.org/10.1080/15376494.2010.499023

[11] W.Zhang, X. Song, X.Gu, S. Li, (2012) Tensile and fatigue behavior of corroded rebars. Constr. Build. Mater., *34*, 409–417. https://doi.org/10.1016/j.conbuildmat.2012.02.071

[12] M.Oyado, T.Kanakubo, T.Sato, Y.Yamamoto, (2011) Bending performance of reinforced concrete member deteriorated by corrosion. Struct. Infrastruct.Eng., 7, 121–130. https://doi.org/10.1080/15732471003588510

[13] D.Proske, S. Hostettler, H.Friedl, (2020) Correction Factors for Collapse Probability of Bridges. Beton Stahlbetonbau,*115*, 128–135. https://doi.org/10.1680/jbren.18.00002

[14] D.Proske, M.Sykora, M.Gutermann, (2020) Correction of failure probability of bridges based on experimental load tests. Bautechnik., 98, 80, https://doi.org/10.1002/cepa.2022

[15] H.W.Song, V. Saraswathy S. Muralidharan, C.H. Lee, K. Thangavel, (2009) Corrosion performance of steel in composite concrete system admixed with chloride and various alkaline nitrites, Corrosion Engineering, Science and Technology, Vol 44 No. 6 . https://doi.org/10.1179/174327809X397848

[16] P.Garces, P.Saura, A.Mendez, E.Zornoza, C.Andrade,(2008) Effect of nitrite in corrosionof reinforcing steel in neutral and acid solutions simulating the electrolytic environments of micropores of concrete in the propagation period, Corrosion science, 50, 498–509 https://doi.org/10.1016/j.corsci.2007.08.016

[17] T.B.Asafa, J.K.Odusote, O.S. Ibrahim, A.Lateef, M.O. Durowoju, M.A. Azeez, T.A.Yekeen, I.C. Oladipo, E.A.Adebayo, J.A.Badmu1, Y.K.Sanusi, O.. Adedokun (2020) Inhibition efficiency of silver nanoparticles solution on corrosion of mild steel, stainless steel and aluminum in 1.0 M HCl medium. IOP Conf. Series: Materials Science and Engineering 805 012018. doi:10.1088/1757-899X/805/1/012018

[18] O.V.Kharissova, H.V. Rasika Dias, B.L. Kharisov, B.Olvera Perez, V.M.Jimenez Perez,(2013) The greener synthesis of nanoparticles. Trends Biotechnol.,31(4) pp 240–248. https://doi.org/10.1016/j.tibtech.2013.01.003

[19] M.Sivaramakrishnan, V.Jagadeesan Sharavanan, D.Karaiyagowder, Y. Meganathan, B.S.Devaraj, S.Natesan, R. Kothandan, K.Kandaswamy,(2019) Green Synthesized Silver Nanoparticles Using Aqueous Leaf Extracts of Leucas Aspera Exhibits Antimicrobial and Catalytic Dye Degradation Properties. SN Appl. Sci., 1. https://doi.org/10.1007/s42452-019-0221-1

[20] P.Taheri, A. Mansouri , B.Bachour, A.Link, N. Ahuja, M.Z. Exova, (2017) Inspection and mitigation of underground corrosion at anchor shafts of telecommunication. NACE,International Corrosion Conference & Expo, pp 72-74

[21] E. Roduner, (2006) Size matters: why nano-materials are different. Chem. Soc. Rev 35(7):583 https://doi.org/10.1039/B502142C

[22] F.Yang, X.Li, Z.Dai, T.Liu W.Zheng H.Zhao, L.Wang, (2017) Corrosion inhibition of poly-dopamine nanoparticles on mild steel in hydrochloric acid solution. Int. J. Electrochem. Sci. 12(8) pp 7469-7480. https://doi.org/10.20964/2017.08.52

[23] D.Abdeen, M. El Hachach, M. Koc, M.Atieh, (2019) A review on the corrosion behaviour of nano-coatings on metallic substrates.Mater 12(2),210. https://doi.org/10.3390/ma12020210

[24] M.Riaz, M.Ismail, B.Ahmad, N.Zahid, G.Jabbour, M.S.Khan, V.Mutreja, S.Sareen, A.Rafiq, M.Faheem (2020) Characterizations and Analysis of the Antioxidant,Antimicrobial, and Dye Reduction Ability

of Green Synthesized Silver Nanoparticles. Green Process. Synth. 9, 693–705. https://doi.org/10.1515/gps-2020-0064

[25] S.Anantharaman, R. Rego, M. Muthakka, T. Anties, H.Krishna, (2020) AndrographisPaniculata-Mediated Synthesis of Silver Nanoparticles: Antimicrobial Properties and Computational Studies. SN Appl. Sci.2 https://doi.org/10.1007/s42452-020-03394-7

[26] S.K.Biswal, M.Behera, A.S.Rout, Tripathy, (2021) A. Green Synthesis of Silver Nanoparticles Using Raw Fruit Extract of Mimusops Elengi and Their Antimicrobial Study. Biointerface Res. Appl. Chem., 11, 10040–10051. https://doi.org/10.33263/BRIAC113.1004010051

[27] S.V. Ganachari, R. Bhat, R. Deshpande, A. Venkataraman, (2012) Extracellular Biosynthesis of Silver Nanoparticles Using Fungi Penicillium Diversum and Their Antimicrobial Activity Studies. BioNanoScience, 2, 316–321. https://doi.org/10.1007/s12668-012-0046-5

[28] S.V. Ganachari, R.Deshpande, R.Bhat, N.V.S Rao, D.S Huh, A.Venkataraman, (2011) Gas Sensing Characteristic of Biofunctionalized Gold Nanoparticles. J. Bionanoscience., 5, 107–112.

[29] S.Rehman, R.Farooq, R.Jermy, S.M.Asiri, V. Ravinayagam, R.Al Jindan, Z. Alsalem,M.A.Shah, Z. Reshi, H. Sabit, (2020) A Wild Fomes Fomentarius for Biomediation of OnePot Synthesis of Titanium Oxide and Silver Nanoparticles for Antibacterial and Anticancer Application. Biomolecules, 10. https://doi.org/10.3390/biom10040622

[30] R.Kavitha, S.Monikandon, D.Kesavan, A.Sankar (2017) Evidence for homogeneous adsorption of samanea saman extract inhibitor on steel surface, Int. J. Chem. Sci., 15(2): 120. doi:10.37273/chesci.cs205310539

[31] S.Monikandon, S.Poongothai, N. Ravisankar, (2024) Biogenic Iron Oxide Nanoparticles As Inhibitor for Corrosion of TMT Rod in Marine Environment, Rasayan J. Chem., 17(2), 688-695, http://doi.org/10.31788/RJC.2024.1728789

[32] S.Sathiyanarayanan, C.Marikkannu N.Palaniswamy (2005) Corrosion inhibition effect oftetramines for mild steel in 1M HCl. Appl. Surf. Sci.241 (3-4) pp 477-484.

[33] https://doi.org/10.1016/j.apsusc.2004.07.050

[34] B.Latha, K.Kavitha,S.Rajendran,(2024)Inhibition of corrosion of mild steel in simulated oil well waterby aqueous extract of Hibiscus rosa-sinensisflower Zastita Materijala 65 (1)86-96. https://doi.org/10.62638/ZasMat1005

[35] T. Velmurugan, A. Divya Sebasthi, S. Thangavel, (2024). Estimation of Primary and Secondary Metabolites and In Vitro Free Radical Scavenging Activities with Ficus tsjahela Burm.F. Crude Extracts in Natural Product Experiments in Drug Discovery, Ed.Karuppusamy Arunachalam, Xuefei Yang, Sreeja Puthanpura Sasidharan.

IZVOD

NHIBICIJA MORSKE KOROZIJE TERMOMEHANIČKI OBRAĐENE ŠIPKE KORIŠĆENJEM ZELENIH SINTETIZOVANIH NANOČESTICA OKSIDA GVOŽĐA

Ova studija istražuje upotrebu nanočestica oksida gvožđa sintetizovanih iz Ficus tsjahelas zaštitnog premaza za termomehanički obrađene (TMT) štapove u morskom okruženju. Metoda je započeta ekstrakcijom inhibitora iz listova biljaka korišćenjem etanola , nakon čega je usledila priprema nanočestica oksida gvožđa. Zatim su (TMT) šipke obložene ovim FeNP-ovima i izložene korozivnim uslovima morskog okruženja. U ovoj studiji nanočestice oksida gvožđa su proizvedene korišćenjem pristupa hemijskom precipitacijom , a efekti veličine čestica su u potpunosti proučavani primenom tehnika kao što su infracrvena spektroskopija Furijeove transformacije (FT-IR), ultraljubičasta vidljiva spektroskopija (UV-Visible) i SEM. Zanimljivo je kada su (TMT) šipke obložene sa 10 slojeva FeNP-a, efikasnost inhibicije korozije porasla je na 94,1% za šipke od 8 mm, 95,4% za šipke od 10 mm i 98,7% za šipke od 16 mm. Štaviše, inhibitivni rezultati su odgovarali Langmuir-ovoj adsorpcionoj izotermi što ukazuje da inhibitorni efekat FeNP-a prati fizički proces adsorpcije.

Ključne reči: *nanočestice, zelene nanočestice, korozija morske strukture, TMT štap Korozija, korozija bočate vode*

Naučni rad
Rad primljen: 19.06.2024.
Rad korigovan: 28.08.2024.
Rad prihvaćen:12.09.2024.

S. Monikandon http://orchid.org/0000-0003-4197-4867
N. Ravisankar http://orchid.org/0000-0002-1762-7358